High-Performance Size Exclusion Chromatography Using Enhanced-Fluidity Liquid Mobile Phases

Huimin Yuan, Isabelle Souvignet, and **Susan V. Olesik***

Ohio State University, Department of Chemistry, 100 West 18th Street, Columbus, OH 43210

Abstract

One of the most effective ways to improve the resolution of size exclusion chromatography (SEC) is to decrease band broadening by lowering the mobile phase viscosity. In this study, the use of enhanced-fluidity liquid mixtures of tetrahydrofuran (THF)–liquid CO_2 for the separation of polystyrene standards by SEC under room temperature and moderate pressure conditions was investigated. By adding low viscosity liquid CO_2 to THF, the mixtures had markedly lower viscosities than THF. As a result, higher efficiency and a shorter analysis time were obtained. When a mixture with 40 mol % CO_2 and 60 mol % THF was used as the mobile phase, the pressure drop across the column decreased by 38% compared with the drop obtained using 100% THF as the mobile phase. Kamlet-Taft solvatochromic parameters π^* and β were used to measure the solvent strength of the THF–CO_2 mixtures. A solvent strength similar to that of pure THF was observed when up to 50 mol % CO_2 was added to THF. No notable deviation in the SEC calibration curve was observed when up to 40 mol % CO_2 was used. However, as a consequence of diminished solvent strength, significant adsorption of solutes to the stationary phase was detected when more than 50 mol % CO_2 was used.

Introduction

Size exclusion chromatography (SEC) is the most common means of determining molecular weight (MW) distributions of natural and synthetic polymers today (1,2). It is also a valuable tool for the cleanup of complex samples before further analysis by other types of chromatography or electrophoresis. SEC was recently evaluated theoretically to be the most suitable method for size-dependent separations of molecules with MWs less than 10^5, compared with thermal field-flow fractionation, packed-column, and open-tubular hydrodynamic chromatographies (3). The retention by SEC is totally controlled by the equilibrium distribution of solute between the bulk solvent and the solvent that occupies the pores (i.e., the separation is

entropy-controlled instead of enthalpy-controlled). Because the solutes are eluted within the total volume of the column, the peak capacity of SEC is relatively low. Because the solvent strength of bulk solvent minimally affects retention or selectivity of SEC, improvement of chromatographic efficiency is the most important way to improve resolution.

Toward this goal, Kirkland (4) developed a new stationary phase that consists of a silica microsphere with a 5-μm solid core and an outer shell (approximately 1-μm-thick) with 300 Å pores. Compared with conventional totally porous particles, such superficially porous particles afforded better mass transfer and an approximately 1.7-fold increase in column efficiency. However, most of the efforts to optimize SEC separations have centered on decreasing the viscosity of the mobile phase. Chromatographic band dispersion is substantially influenced by the viscosity of the solvent because the diffusion coefficient of a solute has an approximate inverse relation to the solvent viscosity. Most of the previous attempts to lower the solvent viscosity involved increasing the column temperature. Takeuchi et al. (5) showed a maximum of an approximately 1.4-fold increase in column efficiency using tetrahydrofuran (THF) mobile phase at 70–100°C; however, the column efficiency decreased when the temperature was raised above 100°C. Renn and Synovec (6) demonstrated a fourfold reduction in analysis time with no significant sacrifice in efficiency using high-speed SEC at 150°C and methylene chloride as the mobile phase. Giddings et al. (7) investigated the use of 1,1-difluoroethane as the mobile phase at up to 1088 atm and at temperatures above the boiling or critical temperature of the mobile phase. Fujimoto et al. (8) studied size exclusion separations using supercritical methylene chloride as the mobile phase at 310 atm and 244°C. In three of these studies (6–8), enhanced efficiency and shorter analysis time were observed in the separation of polystyrene standards and other synthetic polymers. However, increased pressures were necessary to maintain sufficient solvent strength and avoid nonexclusion-type retention interactions. High temperatures may pose problems for thermally sensitive analytes and thermally labile stationary phases; high pressures may affect the physical properties of stationary phases as well.

---

* Author to whom correspondence should be addressed.

An enhanced-fluidity liquid is prepared by mixing a low viscosity liquid, usually liquid CO_2, with a common organic solvent. Enhanced-fluidity liquids have markedly lower viscosities than common organic solvents. For example, the viscosity of THF at 20°C is 0.35 cP, but the viscosity of liquid CO_2 at 25°C and 170 atm is 0.09 cP (9). Therefore, THF–CO_2 mixtures should have substantially lower viscosities than commonly used liquids (10). CO_2 is nonpolar; therefore, increasing proportions of CO_2 will eventually diminish the solvent strength. However, as will be illustrated later, large proportions of CO_2 can be added to THF before a noticeable change in solvent strength occurs. Previous studies illustrated that the use of enhanced-fluidity mixtures of methanol–CO_2 with a glassy carbon stationary phase increased the optimal linear velocity and decreased analysis time and pressure drop (9). The application of methanol–H_2O–CO_2 mixtures in reversed-phase chromatography, augmented with temperature elevation, provided marked increases in the solute diffusion coefficient, a substantial decrease in analysis time, and higher column efficiency (11). Similarly improved performance was also observed in normal-phase chromatography using hexane–CO_2 mixtures as the mobile phase (12).

Herein, we report initial studies on the use of THF–CO_2 liquid mixtures for high-performance size-exclusion separations of polystyrene standards. THF was used as the organic solvent because of its frequent use as the mobile phase for the SEC separation of many polymers. The variation in solvent strength of THF–CO_2 mixtures as a function of added CO_2 was also characterized by measuring the Kamlet-Taft solvatochromic parameters π^* and β.

Experimental

Materials

Supercritical fluid chromatography (SFC)- and supercritical fluid extraction (SFE)-grade CO_2 (Air Products, Allentown, PA) and stabilized analytical reagent-grade THF (99.9% pure) (Mallinckrodt Specialty Chemicals, Paris, KY) were used as received. The test solutes for the chromatograms were polystyrene standards (MW = 382,100 and polydispersivity index $[M_w/M_n]$ = 1.16; MW = 12,600 and M_w/M_n = 1.04; and MW = 2360 and M_w/M_n = 1.08) and styrene that were obtained from Aldrich Chemical (Milwaukee, WI). For calibration curve constructions, polystyrene standards (MW = 2,316,000, 114,200, 59,500, 18,700, and 5120; M_w/M_n = 1.02, 1.04, 1.06, 1.03, and 1.08, respectively) were purchased from SP² Scientific Polymer Products (Ontario, NY). Polystyrene 687 (M_w/M_n = 1.08) and dibutylphthalate (over 99% pure) were obtained from Aldrich Chemical. Di-n-hexylphthalate and di-n-decylphthalate were obtained from Chem Service (West Chester, PA).

Instrumentation

An ISCO 260D syringe pump (ISCO, Lincoln, NE) operated in the constant pressure mode was used as the solvent delivery system. Samples were introduced onto the column using a Valco W-series high-pressure injection valve (Valco Instruments, Houston, TX) with a 200-nL internal injection loop. A Betasil silica column (250 × 4.6-mm i.d., 5-μm particles with 200 Å average pore size) obtained from Keystone Scientific (Bellefonte, PA) was used. The detector was a Spectra 100 variable wavelength ultraviolet–visible (UV–vis) absorbance detector (Spectra-Physics, San Jose, CA) equipped with a capillary flow cell. The flow cell for detection was created by removing the polyimide coating from a 5-mm section of fused-silica tubing (250-μm i.d.; Polymicro Technologies, Phoenix, AZ). The detector excitation wavelength was 254 nm. A fused-silica restrictor (30-μm i.d.) of an appropriate length was used to control the linear velocity of the mobile phase. A Setra model 204 pressure transducer (Setra Systems, Acton, MA) was placed in line after the detector and before the restrictor. The pressure at the end of the column was monitored because the pressure along the column must be maintained above a minimum pressure to avoid the phase separation of the mixture. The chromatographic data were obtained using a THF solution of the test solutes with concentrations of 0.16–16 mg/mL each.

Two syringe pumps were employed for THF–CO_2 mixture preparation. First, a known amount of THF was filled into the empty pump, and then a specific amount of pure CO_2 was transferred to it from the second pump that contained pure CO_2 at a constant pressure of 238 atm. The CO_2 volume that was needed to reach a specific ratio of THF–CO_2 in the pump was calculated based on CO_2 density at 238 atm and the temperature of the syringe pump. The THF–CO_2 mixture was pressurized to 170 atm and allowed to equilibrate for 12 h before use. All chromatographic experiments were performed at 24°C and at an inlet pressure of 170 atm. The experimental conditions used in this work were in the single liquid phase region of the THF–CO_2 phase diagram (H. Yuan and S.V. Olesik. Comparison of enhanced-fluidity and elevated temperature mobile phases for high-performance size exclusion chromatography. *J. Chromatogr. A*, in press.).

The chromatographic data were collected using an EZChrom chromatography data system (Scientific Software, San Ramon, CA) running on an IBM–PC-compatible computer; data were collected at different sampling rates that were controlled by the analysis time of the separation. The data were analyzed using Peakfit 4.0 for Windows (Jandel Scientific, San Rafael, CA). Peak widths at half-height were determined by fitting the experimental data to a Gaussian peak.

The solvent strength of the THF–CO_2 mixture was determined by monitoring the solvatochromic shift of various dyes. A DMS-100 UV–vis spectrophotometer (Varian, Sunnyvale, CA) was used to measure the spectra of the dyes. The absorption spectrum of each dye was obtained using a homemade, stainless steel, high-pressure, optical flow cell with an internal volume of 10 mL and an optical path length of 3.5 cm. The optical path was terminated on each end with cylindrical quartz windows that were 0.69-in. thick with a 1.125-in. diameter (ESCO Products, Oak Ridge, NJ). The optical cell was sealed with Teflon o-rings. The concentration of the dyes used in these studies was approximately 1×10^{-4}M.

Results and Discussion

Solvent strength

In order to maintain the SEC retention mechanism, the solvent strength of the mobile phase is an important factor to

consider. Numerous studies characterized the necessary solvent strength for a given SEC separation. Altgelt and Moore (13) showed that for a solvent to be compatible with the gel, the Hildebrand solubility parameter of the solvent and the gel should be similar. Dawkins (14) also proposed guidelines for choosing solvents in SEC in terms of the Hildebrand solubility parameters, which include the following: when δ_{solute} is less than δ_{gel}, retention mechanisms other than exclusion will be minimized when $\delta_{solvent}$ is greater than δ_{solute}; when δ_{solute} is greater than δ_{gel}, $\delta_{solvent}$ must be greater than δ_{solute} to minimize nonexclusion retention mechanisms. From these guidelines, the solvent strength should be carefully evaluated, relative to that of the solutes and the gel, to achieve optimal SEC performance.

The Hildebrand solubility parameters for THF and polystyrene are 9.1 H (15). Solute solubility is high when the δ values of both solute and solvent are close. Therefore, as long as the solvent strength of the THF–CO_2 mixtures is similar to the solvent strength of THF, nonexclusion retention mechanisms should be minimized. Kamlet-Taft solvatochromic parameters π^* and β were chosen to characterize the solvent strength of the THF–CO_2 mixtures. The Kamlet-Taft parameters are unique in that they provide information on the specific type of molecular-level interaction present. The π^* parameter is a measure of dipolar and polarizability interactions (16), and β is a measure of the hydrogen bond basicity of a solution. The Kamlet-Taft α parameter (a measure of hydrogen bond acidity) was not measured because both solvents have negligible hydrogen bond acidity.

The solvatochromic shift of the *ortho*-nitroanisole (17) UV–vis spectrum was used to measure the π^* values of the THF–CO_2 mixtures using the following equation:

$$\pi^* = \frac{(v_{max} - v_0)}{s} \qquad \text{Eq 1}$$

where v_{max} is the frequency of the absorbance maximum of o-nitroanisole when dissolved in the solvent of interest, v_0 is the frequency of the absorbance maximum for the molecular probe in a reference solvent (typically cyclohexane), and s is a proportionality constant that limits the values of π^* to a range of 0–1 for common solvents. The literature value of s for o-nitroanisole, -2.428 ± 0.195 kilokelvin (kK), was used to calculate π^* in these experiments (18). Cyclohexane was used as the reference solvent. The absorption maximum for o-nitroanisole in cyclohexane was 47.1 kK.

Figure 1A shows the variation of the π^* parameter with THF–CO_2 composition at 25°C and 136 atm. Values of π^* decreased as the mole fraction of CO_2 increased in the mixture. Two negative slopes were observed on the curve. The slope changed significantly at approximately 0.70 mole fraction CO_2 in THF. For mole fractions of CO_2 greater than 0.70, π^* decreased drastically with added CO_2.

The values of the β parameter for the THF–CO_2 mixtures were determined by measuring solvatochromic shift of 4-nitroaniline (A) relative to that of N,N-dimethyl-4-nitroaniline (B) (19). The regression equation for the linear plot of v_{max} (A) for 4-nitroaniline versus the v_{max} (B) of N,N-dimethyl-4-

nitroaniline in solvents that vary in polarity but lack hydrogen bonding capability was then determined:

$$v_{max} (A) = 1.0534 v_{max} (B) - 6.45 \text{ (kK)} \qquad \text{Eq 2}$$

$(r^2 = 0.997)$

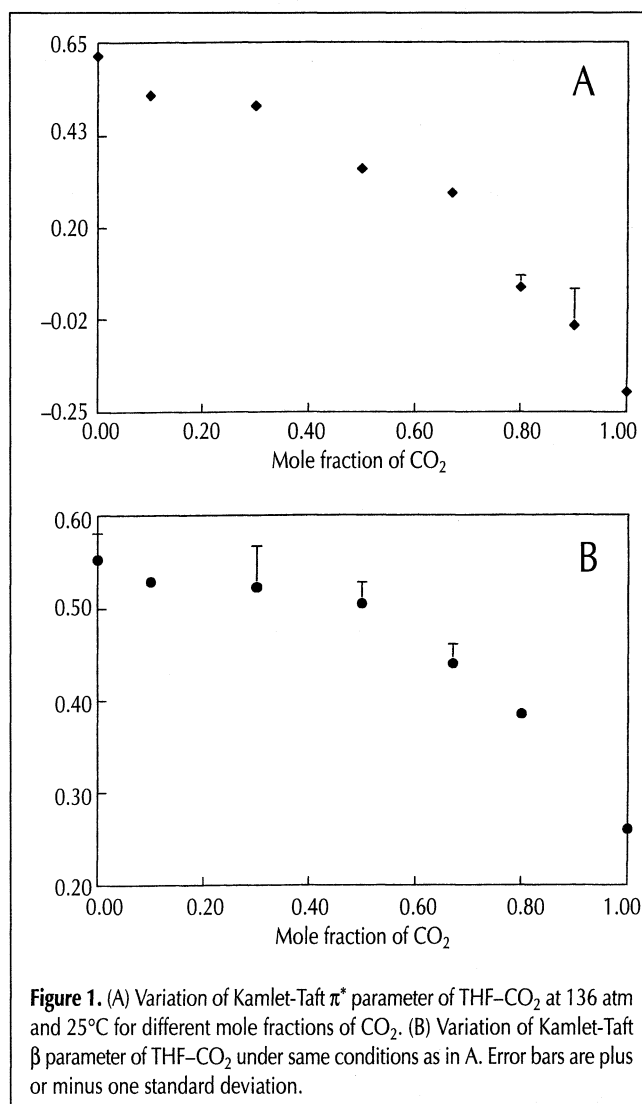$$\Delta\Delta v_{max (A-B)} = v_{max} (1 \, cal) - v_{max} (1 \, exp) \qquad \text{Eq 3}$$

$$\beta = \frac{-\Delta\Delta v_{max(A-B)}}{2.80} \qquad \text{Eq 4}$$

The presence of hydrogen bonding in solvents causes deviation from this line. The extent of deviation was used to calculate the β parameter. β was calculated using Equations 3 and 4: $v_{max} (1 \, cal)$ is the frequency of 4-nitroaniline calculated from Equation 2, and $v_{max} (1 \, exp)$ is the frequency maximum in the solvent of interest (THF–CO_2 mixtures) (19).

Figure 1B shows the variation of the β parameter with THF–CO_2 composition at 25°C and 136 atm. The β parameter, like π^*, decreased as the proportion of CO_2 increased, and a slope change occurred at approximately 0.50 mole fraction CO_2 in THF.

Figure 1. (A) Variation of Kamlet-Taft π^* parameter of THF–CO_2 at 136 atm and 25°C for different mole fractions of CO_2. (B) Variation of Kamlet-Taft β parameter of THF–CO_2 under same conditions as in A. Error bars are plus or minus one standard deviation.

411

In summary, a substantial decrease in solvent strength of the THF–CO_2 mixtures occurred when more than 0.5 mole fraction CO_2 was in the mixture at 136 atm.

Chromatographic band dispersion

A generalized equation describing the possible contributions to chromatographic band dispersion of polymers in SEC is given by (20,21):

$$H_{TOT} = A + \frac{B}{u} + C_f u + C_{sm} u + \frac{\sigma^2_{dist}}{L} \qquad \text{Eq 5}$$

where u is the interstitial linear velocity; A describes the dispersion due to multiple flow paths available to the analyte molecules; B describes the dispersion due to longitudinal diffusion; C_f describes the dispersion due to the presence of a laminar flow profile in the moving fluid; C_{sm} describes the dispersion due to diffusion in the "stationary" fluid within the pore structure; and σ^2_{dist}/L (with units of length) describes the inherent dispersion in the molecular weight distribution of the polymer, where L is the length of the column and σ_{dist} is the standard deviation of the MW distribution. By taking the derivative of Equation 5 with respect to linear velocity and setting the derivative equal to zero, the optimal linear velocity, u_{opt}, is $(B/C)^{1/2}$. Because the B coefficient is a linear function of the solute diffusion coefficient and the C coefficients, C_f and C_{sm}, are inversely related to the solute diffusion coefficient, u_{opt} should vary linearly with the diffusion coefficient.

Under ideal SEC conditions (i.e., no solute–gel interactions), the band dispersion at linear velocities greater than u_{opt} is controlled predominately by the C_{sm} term. For columns packed with spherical particles, C_{sm} may be calculated from Equation 6 (22):

$$C_{sm} = \frac{R(1-R)\, d_p^2}{30\gamma D_{12}} \qquad \text{Eq 6}$$

where the retention ratio $R = V_0/V_r$; V_0 is the interstitial volume, V_r is the retention volume, d_p is the particle diameter, D_{12} is the diffusion coefficient of the analyte molecule in the mobile phase, γ is the obstruction factor, and γD_{12} is the apparent diffusion coefficient in the pores, which is smaller than D_{12} in free fluid due to the presence of the gel pore network. Therefore, at linear velocities greater than u_{opt}, the plate height should decrease as the analyte diffusion coefficient increases. The effect of solvent viscosity and solute molecular weight on the diffusion coefficient of a polymeric solute in the bulk solution is described by (23):

$$D_{12} = \frac{RT}{6\pi\eta N_0} \left(\frac{10\pi N_0}{3K}\right)^{1/3} M^{-(1+a)/3} \qquad \text{Eq 7}$$

where R is the gas constant; T is absolute temperature; η is solvent viscosity; N_0 is Avogadro's number; M is the molecular weight of the polymers; and K and a are constants in the Mark-Houwink equation $[\eta] = KM^a$, where $[\eta]$ is the intrinsic viscosity. The terms K and a are dependent only on the specific polymer-solvent system. Values of K and a for polymers in common liquid solvents are available in the literature (24). Equations 6 and 7 clearly show that lowering solvent viscosity should reduce the chromatographic band dispersion associated with the stationary liquid in the gel pores.

Two test compounds, styrene and the polystyrene standard with an MW of 12,600, were chosen to show the variation of plate height with the linear velocity of the mobile phase. These two compounds represent examples of small molecules and macromolecules, respectively.

Figure 2 shows the reduced plate height versus linear velocity plots for styrene and polystyrene 12,600, using four mobile phase compositions (pure THF, 80:20 THF–CO_2, 70:30 THF–CO_2, and 60:40 THF–CO_2 [mole fraction]) at ambient temperature. The linear velocity was determined based on the retention time of a totally excluded polystyrene peak. The linear velocity range studied was 0–1.0 cm/s. The curves for styrene exhibited the characteristic shape of the van Deemter plot; however, for polystyrene 12,600, the upswing at low mobile phase velocities, which is controlled by the longitudinal diffusion B term, was not observed. This was due to the extremely low diffusion coefficient of polymers compared with small molecules. The B term could only be seen when the mobile phase velocity was extremely low, which is experimentally impractical.

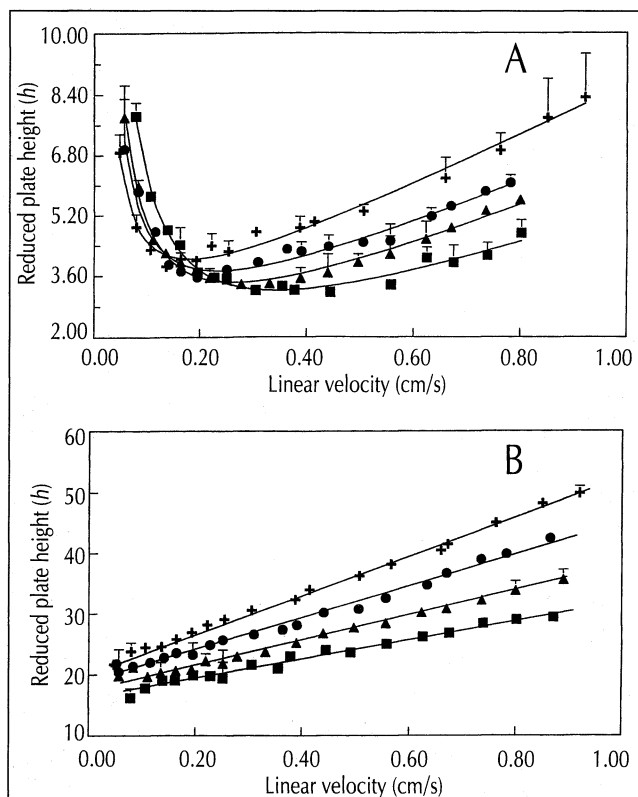For styrene (Figure 2A), the optimal linear velocity (where

Figure 2. Variation of reduced plate height of (A) styrene and (B) polystyrene standard 12,600 with mobile phase linear velocity for different mobile phase compositions at 170 atm and 24°C: pure THF (+), 80:20 THF–CO_2 (mole fraction) (•), 70:30 THF–CO_2 (▲), and 60:40 THF–CO_2 (■). Each value is an average of triplicate determinations. Error bars signify plus or minus one standard deviation.

the lowest plate height was obtained) increased as the proportion of CO_2 in the THF–CO_2 mixture increased. The value of the plate height at the optimal linear velocity also decreased with increasing proportions of CO_2. In addition, for any linear velocity greater than u_{opt}, the plate height was the smallest for the mixture containing the highest amount of CO_2. Because polydispersity does not apply to styrene, the curves were fit to the van Deemter equation $H = A + B/u + Cu$. Squares of the correlation coefficients (r^2) for all the curves were greater than or equal to 0.98. The constants A, B, and C and their 95% confidence intervals for the four mobile phase compositions are listed in Table I. The A term decreased to values close to zero when CO_2 was in the mixture. The B term, representing the dispersion due to longitudinal diffusion, increased with higher CO_2 proportions. Therefore, faster longitudinal diffusion of the solute was indicated when low viscosity CO_2 was added into the mobile phase. The C term, which was inversely proportional to the solute diffusion coefficient, decreased with higher CO_2 percentages. Accordingly, faster mass transfer of the solute within the pore structure of the stationary phase occurred with increasing CO_2. Compared to pure THF, the use of 40:60 CO_2–THF mobile phase dropped the C term to 74% of the original value.

The van Deemter curves for the polystyrene standard with an MW of 12,600 resembled the curves for styrene at regions where the linear velocity u was greater than u_{opt}. The plate height at any linear velocity decreased with the addition of CO_2. The H versus u curves were roughly linear, and the slope should be approximately equal to the C_{sm} term. The least-squares fit of the data points for each mobile phase to a straight line gave r^2 values greater than or equal to 0.98. The calculated C terms are summarized in Table I. The C term for the 60:40 THF–CO_2 was 51% less than the term obtained when THF was the mobile phase.

Pressure drop

Darcy's Law (25) predicts a linear relationship between solvent viscosity (η) and the pressure drop (ΔP) across a packed column:

$$\Delta P = \frac{\phi \eta <u> L}{d_p^2} \qquad \text{Eq 8}$$

where ϕ is a dimensionless flow resistance parameter; $<u>$ is

the average linear velocity, L is the length of the column, and d_p is the diameter of the particle. Figure 3 shows the variation in pressure drop versus linear velocity for the four THF–CO_2 mixtures with CO_2 mole fractions of 0–40%. The linear relationship between pressure drop and linear velocity indicated the silica stationary phase was rigid with minimal compressibility under all the conditions tested. At any linear velocity, the pressure drop across the column decreased with higher proportions of CO_2, which reflected the fluidity enhancement of liquid CO_2. Because $\phi L/d_p^2$ was a constant in the present study, the variation in the slope of the curves represented the change in the viscosity of the four mobile phases. By adding 20, 30, and 40 mol % CO_2 to the mobile phases, the viscosity was lowered by approximately 23, 29, and 42%, respectively. The limited peak capacity of SEC often requires the use of two to five SEC columns connected in series to effectively separate a polymer mixture. The low pressure drop achieved with these enhanced-fluidity mixtures allowed more columns to be placed in series to obtain even higher efficiency than presently possible.

Analysis time

The chromatographic variables that control the time of analysis for SEC separation of a polymer mixture are shown in
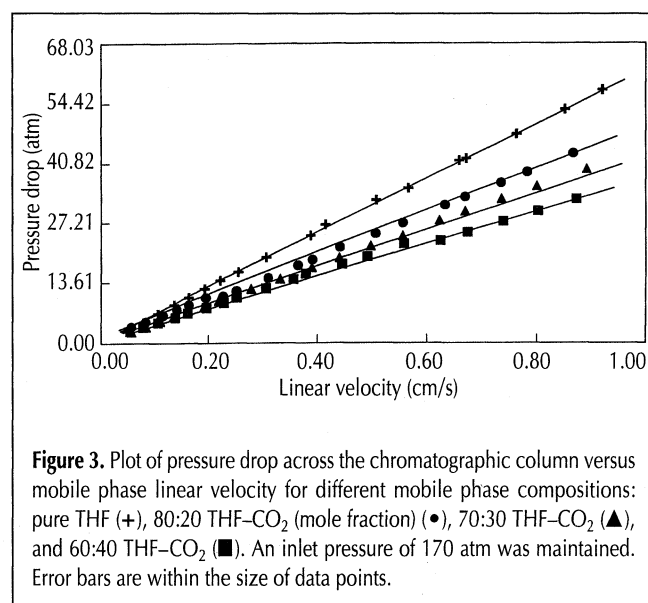

Figure 3. Plot of pressure drop across the chromatographic column versus mobile phase linear velocity for different mobile phase compositions: pure THF (+), 80:20 THF–CO_2 (mole fraction) (●), 70:30 THF–CO_2 (▲), and 60:40 THF–CO_2 (■). An inlet pressure of 170 atm was maintained. Error bars are within the size of data points.

Table I. Variation in van Deemter Equation Coefficients for Styrene and Slopes in Figure 2B for Polystyrene Standard 12,600 with the Mobile Phase Composition

Mobile phase composition	Styene				PS 12,600
	$A \times 10^{-3}$ (cm)	$B \times 10^{-3}$ (cm²/s)	$C \times 10^{-3}$ (s)	$H/u^* \times 10^{-3}$ (s)	$C^\dagger \times 10^{-3}$ (s)
THF	7.6 ± 0.3	1.2 ± 0.2	3.5 ± 0.4	5.2	15.7 ± 0.5
80:20 THF–CO_2	0.4 ± 0.2	1.7 ± 0.2	3.0 ± 0.4	4.4	13.0 ± 0.7
70:30 THF–CO_2	0.2 ± 0.2	2.1 ± 0.2	2.9 ± 0.3	4.0	9.8 ± 0.6
60:40 THF–CO_2	-0.2 ± 0.1	3.1 ± 0.3	2.6 ± 0.4	3.3	7.9 ± 0.6

* Calculated at a linear velocity of approximately 0.5 cm/s.

† Slopes of the fitted line in Figure 2B.

Equation 9 (23).

$$t_r = \frac{16H}{S^2 \left(\dfrac{\Delta M}{M}\right)^2 u} \left(1 + \frac{K_{SEC} V_p}{V_0}\right) \qquad \text{Eq 9}$$

M is the molecular weight of the polymer, S is the column selectivity, which can be described as the absolute value of $d[\log t_r]/d[\log M]$, ΔM is the molecular weight interval that must be resolved at unit resolution, K_{SEC} is the distribution coefficient, and V_p is the stationary phase volume or pore volume. The other variables were defined previously. According to Equation 9, H/u should be minimized to shorten the analysis time. H/u values for styrene with the four different

Figure 4. Chromatograms of the separations of four analyses, polystyrene standards 382,100 (peak 1); 12,600 (peak 2); 2,360 (peak 3); and styrene (peak 4) using three mobile phase compositions: (A) pure THF, (B) 70:30 THF–CO$_2$, and (C) 60:40 THF–CO$_2$ at 24°C. A flow rate of 0.90 mL/min was maintained by adjusting the restrictor length.

mobile phases at a linear velocity of 0.5 cm/s are listed in Table I. Because the H/u plot for polystyrene 12,600 is almost a straight line, the slope is proportional to the analysis time. For both styrene and the polystyrene polymer, adding CO_2 into THF clearly lowered the analysis time. When the analysis time with pure THF was compared with that of 60:40 THF–CO$_2$, the latter showed a 40–50% decrease in analysis time for styrene and polystyrene 12,600. The time of analysis should continue to decrease when more CO_2 is added until the selectivity of the separation is affected by the decreasing solvent strength of the mobile phase.

Chromatograms

Figure 4 shows the separations of four analytes (polystyrene standards 382,100; 12,600; 2360; and styrene) at the same flow rate but using four different mobile phase compositions. The flow rate was adjusted to approximately 0.9 mL/min by varying the restrictor length. The pressure drop across the column is provided along with the number of theoretical plates for the analytes, except for polystyrene 382,100, whose peak was significantly tailed due to its larger polydispersity ($M_w/M_n = 1.16$). The plate numbers of polystyrene 12,600 and 2,360 are in the same range and are shown as the average of the two. Higher plate numbers were observed when higher proportions of CO_2 were added. For instance, the plate numbers for polymers (polystyrene 12,600 and 2,360) and styrene increased 1.8-fold and 1.6-fold, respectively, by adding 40% CO_2 to THF. Although the highest efficiencies were attained when 40% CO_2 was used, baseline resolution was lost between polystyrene 2,360 and styrene. This was caused by the gradual reduction of solvent strength of the mobile phase when more CO_2 was added at this inlet pressure. In fact, the solvent strength can be maintained by employing higher pressures. Because this was not the emphasis of our study, the pressures that can maintain sufficient solvent strength and recover the resolution were not investigated. Nevertheless, the size exclusion mechanism is still the dominant mechanism at 40% CO_2 mole fraction.

Changes in the chromatography resulting from the addition of CO_2 into the mobile phase are more clearly seen in Figure 5. At the constant inlet pressure of 170 atm, the restrictor length was held constant, which caused the linear velocity to vary with the four different mobile phase compositions (pure THF, 80:20, 70:30, and 60:40 THF–CO$_2$). The viscosity reduction was reflected in the faster flow rate observed. The flow rate was monitored directly from the syringe pump. From pure THF to the 60:40 THF–CO$_2$ mixture, the flow rate increased by 74%; the elution time of styrene was shortened from more than 9 min to less than 6 min.

However, when more than 40% mole fraction of CO_2 was added, the nonexclusion mechanism appeared to contribute significantly. Figure 6 shows the separation of four analytes at a constant flow rate of approximately 0.9 mL/min using 50:50 and 40:60 THF–CO$_2$ mixtures as mobile phases. Although the elution was still in the order of decreasing molecular weight, the last three peaks were poorly resolved when 50% CO_2 was used because the retention time of polystyrene 12,600 and 2,360 increased significantly. The peak height for the highest
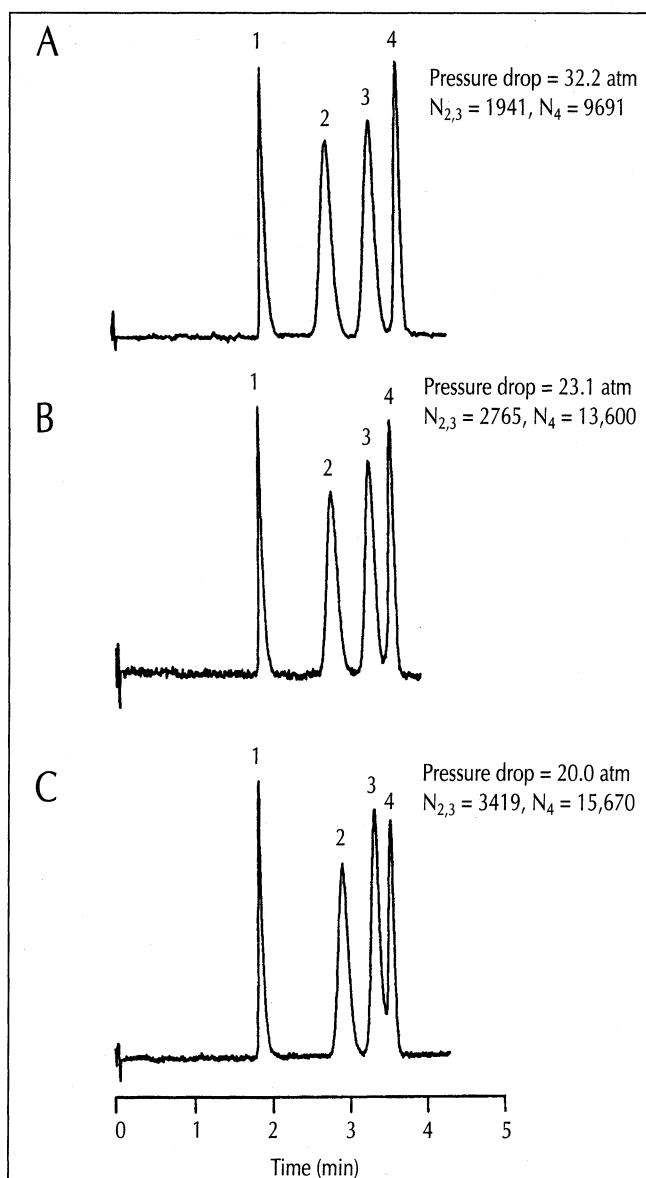
Figure 5. Chromatograms of the separations of four analyses, polystyrene standards 382,100 (peak 1); 12,600 (peak 2); 2,360 (peak 3); and styrene (peak 4) using four mobile phase compositions: (A) pure THF, (B) 80:20 THF–CO$_2$, (C) 70:30 THF–CO$_2$, and (D) 60:40 THF–CO$_2$ under the same restrictor (30-μm i.d., fused silica) length of 10 cm. The flow rates for the conditions were read directly from the syringe pump: (A) 0.34 mL/min, (B) 0.45 mL/min, (C) 0.50 mL/min, and (D) 0.59 mL/min.

Figure 6. Chromatograms of the separations of four analyses, polystyrene standards 382,100 (peak 1); 12,600 (peak 2); 2,360 (peak 3); and styrene (peak 4) using the mobile phase compositions of (A) 50:50 THF–CO$_2$ and (B) 40:60 THF–CO$_2$. A flow rate of 0.90 mL/min was maintained by adjusting the restrictor length. In Figure 6B, polystyrene 382,100 did not elute.
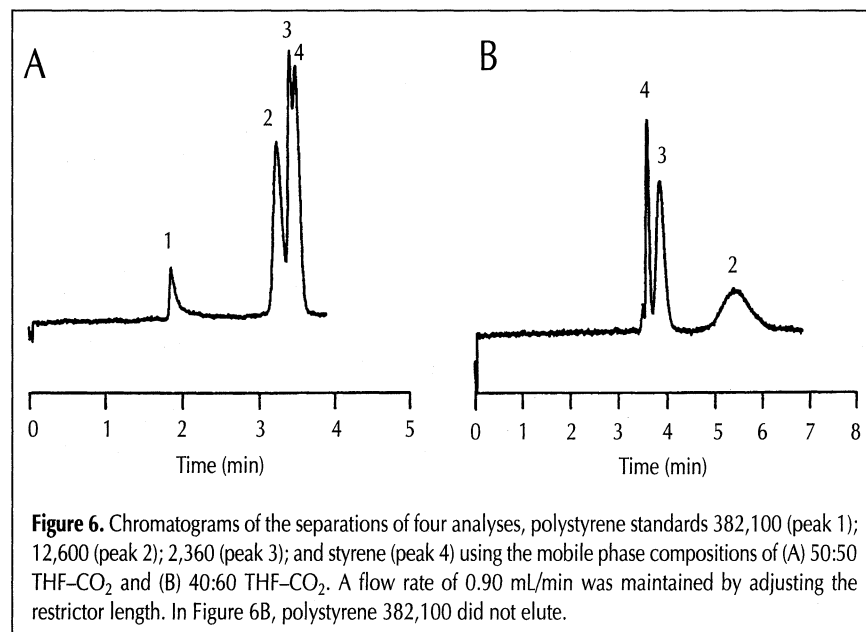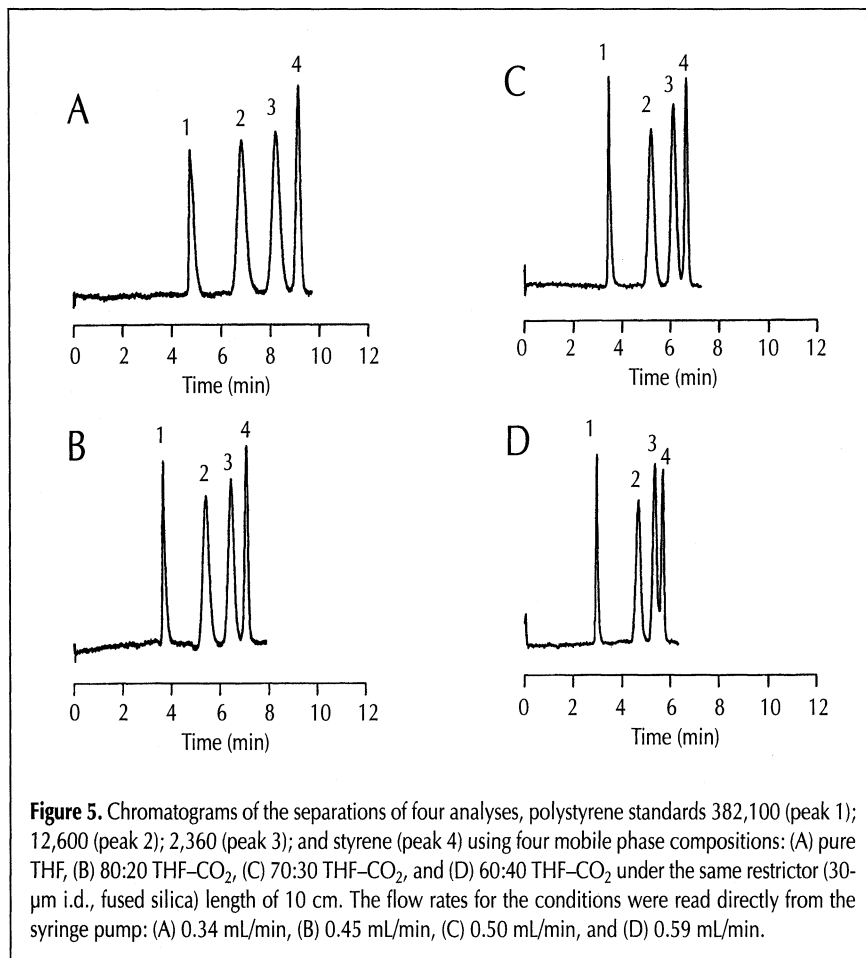
MW calibration curves

When size exclusion is the controlling retention mechanism for a given separation, retention volume for a given analyte can be used to determine its MW. Calibration plots of MW versus retention volume using polymers of known MW and low polydispersivity, such as the polystyrene standards used in this study, allow the MW determination of unknown polymers. The curves on these plots should be unaffected by solvent composition unless interaction mechanisms other than size exclusion contributed to retention. MW calibration curves using 13 different MW standards, ranging from polystyrene with an M$_W$ of 2,316,000 to styrene, and four mobile phase compositions are shown in Figure 7. Under the constant inlet pressure of 170 atm, the restrictor length was adjusted to maintain the flow rate around 0.9 mL/min for different mobile phase compositions. The retention volume for each analyte was determined by multiplying the retention time by the flow rate. The measured flow rate variation was ± 0.005 mL/min, which minimally affected the measured retention volume. Each data point was the average of duplicate determinations. As revealed on the plot, the MW standards chosen covered the range of total exclusion to total pore penetration.

The calibration curves for the four mobile phases, pure THF, 80:20, 70:30, and 60:40 THF–CO$_2$ mixtures, exhibited globally similar shapes and almost overlapped with the same linear calibration range (MWs of approximately 2,360 to 59,500). The resemblance of the calibration curves using THF–CO$_2$ mixtures with up to 40% CO$_2$ mole fraction to the calibration curve with pure THF indicated that the THF–CO$_2$ mixtures used here maintained sufficient solvent strength to keep the size exclusion mechanism dominant. However, slight differences in retention volumes were seen for different mobile phases, especially in the linear calibration range. Higher CO$_2$ mole fractions showed slightly prolonged retention volumes, implying subtle adsorption accompanying the CO$_2$ addition. Negligible variation in pore volume (1.59–1.62 mL) was observed for the four mobile phases, which indicated minimal change in the support material when the enhanced-fluidity liquid mixtures were used as mobile phases.
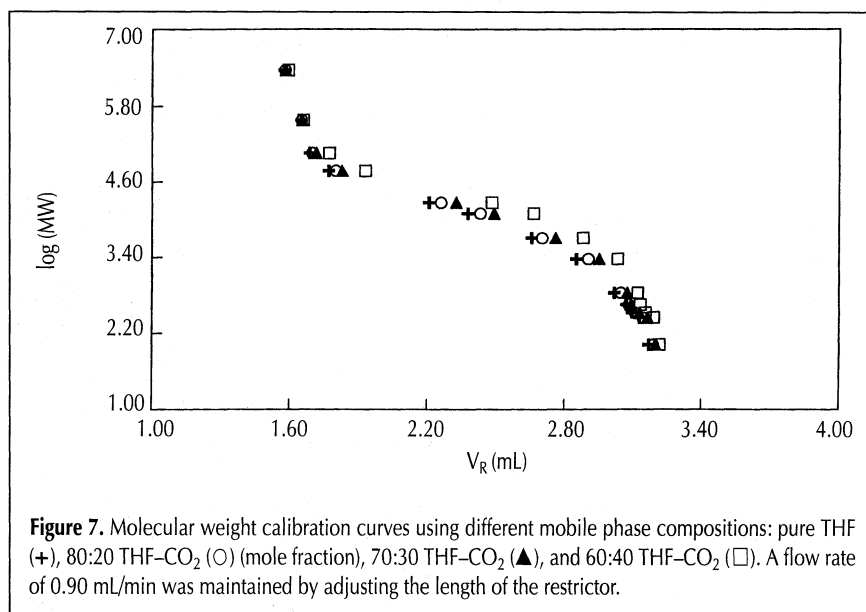
molecular weight polymer, polystyrene 382,100, decreased dramatically due to its adsorption onto the stationary phase. The deviation from the size exclusion mechanism increased when 60% CO$_2$ mole fraction was used, the elution order was reversed, and polystyrene 382,100 did not elute from the column due to strong adsorption.

Figure 7. Molecular weight calibration curves using different mobile phase compositions: pure THF (+), 80:20 THF–CO_2 (O) (mole fraction), 70:30 THF–CO_2 (▲), and 60:40 THF–CO_2 (□). A flow rate of 0.90 mL/min was maintained by adjusting the length of the restrictor.

Conclusion

The addition of liquid CO_2 to THF is an efficient means of reducing the viscosity of the mobile phase for SEC. The chromatographic efficiency increased with higher proportions of CO_2, and the optimal linear velocity also shifted to higher values as predicted theoretically. The viscosity reduction was also reflected in a lower pressure drop across the column (62% of the original by using 40% CO_2) and shorter analysis times were observed. According to MW calibration curves and spectroscopic studies, the solvent strength of the THF–CO_2 mixture at 170 atm was maintained when as much as 40% CO_2 was added. Higher CO_2 proportions resulted in an onset of significant nonexclusion interactions at the experimental pressure. Finally, the improvement of SEC performance by using enhanced-fluidity liquid mobile phases can be further complemented with stationary phase modification, such as using superficially porous silica microspheres (4) or smaller particles.

Acknowledgments

References

1. *Chromatography of Polymers: Characterization by SEC and FFF.* T. Provder, Ed. ACS Symposium series 521, American Chemical Society, Washington, DC, 1993.
2. *Steric Exclusion Liquid Chromatography of Polymers.* J. Janča, Ed. Marcel Dekker, Inc., New York, NY, 1984.
3. G. Stegeman, A.C. van Asten, J.C. Kraak, H. Poppe, and R. Tijssen. Comparison of resolving power and separation time in thermal field-flow fractionation, hydrodynamic chromatography, and size-exclusion chromatography. *Anal. Chem.* **66:** 1147–60 (1994).
4. J.J. Kirkland. Superficially porous silica microspheres for the fast high-performance liquid chromatography of macromolecules. *Anal. Chem.* **64:** 1239–45 (1992).
5. T. Takeuchi, S. Matsuno, and D. Ishii. Temperature effects in microcolumn size exclusion chromatography. *J. Liq. Chromatogr.* **12:** 987–96 (1989).
6. C.N. Renn and R.E. Synovec. Effect of temperature on separation efficiency for high-speed size exclusion chromatography. *Anal. Chem.* **64:** 479–84 (1992).
7. J.C. Giddings, L.M. Bowman, and M.N. Myers. Exclusion chromatography in dense gases: An approach to viscosity optimization. *Anal. Chem.* **49:** 243–49 (1977).
8. C. Fujimoto, T. Watanabe, and K. Jinno. Size exclusion chromatography of polystyrenes with supercritical dichloromethane. *J. Chromatogr. Sci.* **27:** 325–28 (1989).
9. Y. Cui and S.V. Olesik. High-performance liquid chromatography using mobile phases with enhanced fluidity. *Anal. Chem.* **63:** 1812–19 (1991).
10. R.C. Reid, J.M. Prausnitz, and B.E. Poling. *The Properties of Gases and Liquids,* 4th ed. McGraw-Hill Book Company, New York, NY, 1987.
11. S.T. Lee and S.V. Olesik. Comparison of enhanced-fluidity and elevated-temperature mobile phases in reversed-phase high-performance liquid chromatography. *Anal. Chem.* **66:** 4498–4506 (1994).
12. S.T. Lee and S.V. Olesik. Normal-phase high-performance liquid chromatography using enhanced-fluidity liquid mobile phases. *J. Chromatogr. A* **707:** 217–24 (1995).
13. K.H. Altgelt and J.C. Moore. *Polymer Fractionation.* M.J.R. Cantow, Ed. Academic Press, New York, NY, 1967, chapter B4.
14. J.V. Dawkins. Polymer–gel interactions in GPC with organic eluents. *J. Liq. Chromatogr.* **1:** 279–89 (1978).
15. A.F.M. Barton. *Handbook of Solubility Parameters and Other Cohesion Parameters.* CRC Press, Boca Raton, FL, 1983.
16. C. Laurence, P. Nicolet, M.T. Dalati, J.-L.M. Abboud, and R. Notario. The empirical treatment of solvent-solute interactions: 15 years of π^*. *J. Phys. Chem.* **98:** 5807–16 (1994).
17. P.C. Sadek, P.W. Carr, R.M. Doherty, M.J. Kamlet, R.W. Taft, and M.H. Abraham. Study of retention processes in reversed-phase high-performance liquid chromatography by the use of the solvatochromic comparison method. *Anal. Chem.* **57:** 2971–78 (1985).
18. M.J. Kamlet, J.L. Abboud, and R.W. Taft. The solvatochromic comparison method. 6. The π^* scale of solvent polarities. *J. Am. Chem. Soc.* **99:** 6027–38 (1977).
19. M.J. Kamlet and R.W. Taft. The solvatochromic comparison method. I. The β-scale of solvent hydrogen-bond acceptor (HBA) basicities. *J. Am. Chem. Soc.* **98:** 377–83 (1976).
20. J.C. Giddings and K.L. Mallik. Theory of gel filtration (permeation) chromatography. *Anal. Chem.* **38:** 997–1000 (1966).
21. J.V. Dawkins and G. Yeadon. High-performance gel permeation chromatography of polystyrene with silica microspheres. *J. Chromatogr.* **188:** 333–45 (1980).
22. J.C. Giddings. *Advances in Chromatography,* Vol. 20. J.C. Giddings, E. Grushka, J. Cazes, and P.R. Brown, Eds. Marcel Dekker, Inc., New York, NY, 1982.
23. A. Rudin and H.K. Johnston. Diffusion coefficients and intrinsic viscosities of polymers. *J. Polym. Sci. Part B.* **9:** 55–60 (1971).
24. J. Brandup and E.H. Immergut, *Polymer Handbook.* John Wiley & Sons, New York, NY, 1975.
25. A.E. Scheidegger. *The Physics of Flow Through Porous Media.* The MacMillan Company, New York, NY, 1960, pp. 68.